HHS Public Access

Author manuscript

Microelectron Eng. Author manuscript; available in PMC 2018 September 27.

Published in final edited form as:

Microelectron Eng. 2018 August 5; 195: 50–56. doi:10.1016/j.mee.2018.03.019.

Droplet Impinging Behavior on Surfaces with Wettability Contrasts

Bahador Farshchian[1], **Jacoby Pierce**[1], **Mohammad S. Beheshti**[2], **Sunggook Park**[2], and **Namwon Kim**[1,3]

[1]Ingram School of Engineering, Texas State University, San Marcos, TX 78666, USA

[2]Department of Mechanical and Industrial Engineering, Center for Bio-Modular Multiscale Systems for Precision Medicine, Louisiana State University, Baton Rouge, LA 70803, USA

[3]Materials Science, Engineering, and Commercialization, Texas State University, San Marcos, TX 78666, USA

Abstract

Heterogeneous substrates with moderate and extreme wettability contrasts were fabricated by comprising of superhydrophobic/hydrophilic and superhydrophobic/extremely hydrophilic surfaces, respectively. The interactions of water droplets impinging on the surfaces with sharp wettability contrasts were investigated experimentally. The impinging droplets that slightly touch the hydrophilic or extremely hydrophilic areas on each substrate exhibit a directional rebounding towards the more wetting surfaces, i.e., hydrophilic or extremely hydrophilic surface. The trajectory and landing distance of the rebounded droplets were tailored by controlling the releasing height of the droplet, wetting contrast across the border, and portion of the droplet touching the more wetting surface of the substrates with wettability contrasts. The landing distance of the droplet increases with the increased releasing height and higher wettability contrast across the border. Increasing the portion of the impinging droplet touching the more wetting surface of the heterogeneous substrates leads to the shorter landing distance of rebounded droplets.

Graphical Abstract

Correspondence to: Namwon Kim.

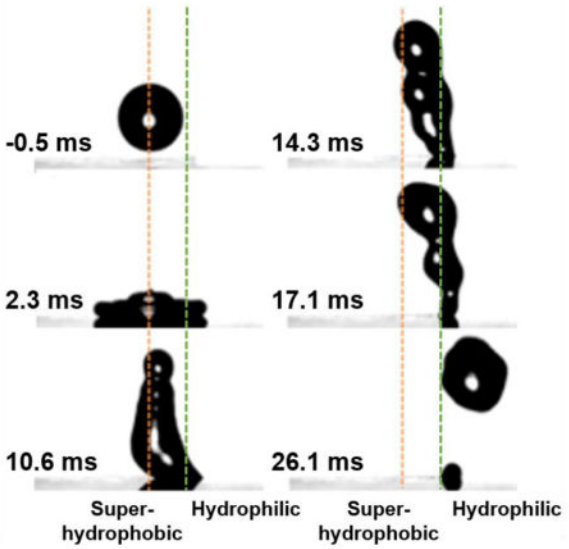

Keywords

droplet impingement; directional rebounding; wettability contrast; heterogeneous; superhydrophobic; hydrophilic

1. Introduction

The study of the interactions of the liquid droplet with a solid surface upon impingement is of practical importance for technical applications such as ink-jet printing, self-cleaning, spray coating, spray cooling, precision solder-drop dispensing, and microfluidics [1–6]. The interaction of liquid droplets with solid surfaces has been studied experimentally and theoretically over the past decades extensively [7, 8]. The dynamic behavior of the impinging droplet is influenced by several parameters, including droplet diameter, impact velocity, droplet liquid material and the wettability property of the substrate, which is controlled by the surface chemistry and surface topography [7]. Most studies on the droplet liquid impingement on solid surfaces are confined to the surfaces with homogeneous wetting properties and fundamental understanding of the droplet impingement on surfaces with heterogeneous wetting properties still limited.

Thanks to the recent advancements in micro- and nanofabrication technologies, various substrates with tailored surface topography and chemistry have been fabricated and employed for droplet manipulation [9–11]. A nanostructured polydimethylsiloxane (PDMS) surface covered by a hard photoactive metal-oxide thin film was fabricated based on a titania layer deposited by atomic layer deposition (ALD) on an aluminum template. The nanostructured hybrid PDMS/titania surface showed robust superhydrophobicity with a combination of comprehensive robustness and self-healing properties [12]. Another robust and self-healing superhydrophobic poly(ethylene terephthalate) (PET) fabric was fabricated using dip-coating of the fabric in a solution of PDMS and octadecylamine (ODA). The superhydrophobic PDMS/ODA-coated PET fibers retained its superhydrophobicity even

after repeated machine washes and various abrasion damages [13]. A droplet gently placed on surfaces with a wettability gradient moves toward the higher wettability region if it overcomes the resistive forces due to the contact angle hysteresis and viscosity [14–16]. The reported studies of the interaction of the liquid droplet with surfaces with a wettability gradient have been mostly limited to the non-impact transport of the droplet on the surface. Sivakumar et al. studied the impact of high-inertial droplets on a textured surface consisting of square-top asperities and reported that the surface textures affect the spreading pattern of the impacting droplets [17]. For the droplet impacting on the hydrophobic grooved surface, it has been demonstrated that the impacting droplet forms a larger contact diameter on the surface in the direction parallel to the groove compared to the direction perpendicular to the groove [18]. Lee et al. demonstrated that thin spokes or narrow fans of liquid can be generated by the drop impact on surfaces with microscale wettability patterns in which hydrophilic (hydrophobic) microscale spokes radiate from the center on a hydrophobic (hydrophilic) background [9]. Malouin et al. investigated the impact of the liquid drop on solid textured surfaces with pillars whose density changed gradually over the surface [10]. Their studies showed a droplet impacting vertically on the surface experiences a transfer of vertical momentum to horizontal momentum toward the more wetting region. The morphing and vectoring of droplets impinging on the surfaces with wettability patterns consisting of hydrophilic/superhydrophilic annulus patterns on a superhydrophobic background was also reported by Schutzius et al. [19] and Kim et al. [11]. Mock et al. studied the impact of the droplet on horizontal and inclined chemically-structured surfaces consisting of hydrophilic spots on a hydrophobic background [20]. Their studies showed that if the impacting droplet during the primary spreading touches the hydrophilic area, its center of gravity reaches the hydrophilic spot. Lim et al. also investigated the evolution of the micro-sized droplet upon impingement on a surface with sharp wettability contrast consisting of hydrophilic lines on a hydrophobic background [21]. In their studies, the ratio of the line width to the initial droplet diameter and the contact angle of the hydrophilic lines were identified as the key factors affecting the conformity of the droplet to the hydrophobic line pattern.

In this paper, we report the results of an experimental study on the dynamic behavior of impinging droplets on surfaces with extreme and moderate wettability contrasts. The surface portions possess different wetting properties, namely superhydrophobic–hydrophilic or superhydrophobic–extremely hydrophilic separated by a sharp borderline, which created substrates with moderate and extreme wettability contrasts.

2. Materials and Methods

In order to create substrates with wettability contrasts, 9.5 cm × 4.5 cm pieces of poly-methyl methacrylate (PMMA) were cut from a sheet of PMMA using a band saw. To fabricate a substrate with moderate wettability contrast (see figure 1a–c), half of the PMMA substrate was covered by a mask and its other half was treated by polydimethylsiloxane (PDMS) coated nanoparticles. To treat the unmasked area with nanoparticles, the surface was coated by a 3 wt% solution of nanoparticles in ethanol and after solvent evaporation at furnace at 80 °C, it was sandwiched between two brass plates and subsequently pressed in a hot press (Carver-3893, Carver, IN) to embed the nanoparticles into the surface. To press the PMMA substrate against the brass plates, the stack of PMMA and brass plates were initially

preheated at 140 °C for 10 minutes and then pressed at 140 °C for 2 minutes at 23 bar. After pressing was accomplished, the stack was cooled down to 70 °C for the PMMA substrate to be separated from the brass plates. The flange around the pressed PMMA was then removed and the edges were sanded using a fine bit belt sander. To fabricate a substrate with extreme wettability contrast (see figure 1d–f), the entire surface of PMMA was initially coated by hydrophobic nanoparticles as explained above. After this, half of the PMMA substrate was activated by oxygen plasma using a plasma cleaner (PDC-32G, Harrick Plasma, NY) at high power and at 400 mTorr pressure for 2 minutes, while the other half was covered by a mask. Surface topographies of the different regions of the substrates were observed by scanning electron microscope (SEM) (400 Helios Nano Lab, FEI, OR). Static contact angles of 5 μL water droplets resting on homogeneous regions of the substrates were measured using a contact angle analyzer (Falcon, First Ten Angstroms, VA). Five measurements were taken to calculate the average contact angle for each region.

Figure 2a illustrates the schematic of the experimental setup used to capture images of the droplets impinging on substrates with moderate (superhydrophobic–hydrophilic) and extreme wettability contrasts (superhydrophobic–extremely hydrophilic). The droplets were impinged at a lateral offset with respect to the borderline (Figure 2b). The substrates with moderate/extreme wettability contrast were mounted on a linear 3 axis translation stage to control the precise position of the releasing height and offset distance. In order to ensure the precise lateral offset distance of the droplet impingement, after a mark of the substrate at the boundary line between two surfaces with wettability contrast was aligned with the center of needle, the substrate was moved along the x-direction using the translation stage. The distance reading from the translation stage was confirmed by image processing using ImageJ (NIH, Bethesda, MA). Distilled water stored in a glass syringe was dispensed through a flat-tipped hypodermic needle with the aid of an automated precise fluid dispensing system (Falcon, First Ten Angstroms, VA). The size of the released droplets was measured from the image of the droplet and was estimated as 2.3 mm. The releasing height was varied in the range 10.5 mm – 30.5 mm to control the Weber number $We = \rho V^2 D/\sigma$ and Reynolds number $Re = \rho VD/\mu$, where ρ is the density, V is the impact velocity, D is the diameter of the impinging droplet, σ is the surface tension, and μ is the dynamic viscosity of water. The ranges of We and Re for droplet impingements are 3 – 19 and 830 – 1,990, respectively. A high-speed camera (NX4-S2, IDT, FL) and a strobe lamp in the backlighting mode (Constellation 60, Veritas, FL) were used to capture different stages of the impinging droplet dynamics at 3,980 fps. The entire setup was established on top of a floating optical table. Image processing was conducted using MATLAB to track the trajectory of the droplet following impingement.

3. Results and Discussion

The images of the water droplets resting on the substrates with wettability contrasts are illustrated in figure 3. In the substrate shown in Figure 3a, the plain PMMA and PMMA treated with hydrophobic nanoparticle areas are separated by a borderline, while the substrate demonstrated in Figure 3b consists of two neighboring areas in which one area is only treated with hydrophobic nanoparticles and the other area is also exposed to oxygen plasma after being treated by hydrophobic nanoparticles. The static contact angles of water

droplets (θ) on plain PMMA, PMMA treated with hydrophobic nanoparticles and PMMA treated with hydrophobic nanoparticles and oxygen plasma were measured to be 83 ± 2°, 164 ± 5° and 9 ± 1°, respectively. The differences in the measured static contact angles between the neighboring areas on the substrates shown in Figures 3a and b creates substrates with moderate ($\Delta\theta$ = 81°) and extreme ($\Delta\theta$ = 155°) wettability contrasts.

Figure 3a and b also depict the SEM pictures of the surface topography of the substrates with moderate and extreme wettability contrasts, respectively. In the substrate with moderate wettability contrast (Figure 3a), the untreated PMMA has a smooth surface whereas the area treated with hydrophobic nanoparticles has a hierarchical roughness. In the area treated by nanoparticles, the combination of high surface roughness and hydrophobicity of the coated nanoparticles create a surface with extreme water repellent properties (θ = 164 ± 5°). In contrast, the untreated area exhibits hydrophilicity, which is due to the hydrophilic nature of the pristine PMMA (θ = 83 ± 2°). In Figure 3b, the portion of the substrate with extreme wettability contrast, which is treated with hydrophobic nanoparticles and then exposed to oxygen plasma, can be compared with its adjacent area, which is only treated by hydrophobic nanoparticles. As the result of the oxygen plasma treatment, the relatively loose nanoparticles are removed from the surface, but the surface still maintains its hierarchical roughness. The high surface roughness coupled with the formation of hydrophilic polar groups on surface as the result of plasma treatment causes the surface to become extremely hydrophilic (θ = 9 ± 1°).

The interaction of water droplets impinging on surfaces with homogeneous wetting properties, including PMMA treated by hydrophobic nanoparticles (superhydrophobic), plain PMMA (hydrophilic) and PMMA treated by hydrophobic nanoparticles and exposed to oxygen plasma, when the droplet is released from height of 30.5 mm are shown in Figure 4. On a homogeneous superhydrophobic surface, the impinging droplet spreads, recoils and rebounds vertically off the surface. For a surface with homogeneous hydrophilic surface, the droplet sticks and oscillates on the surface, while it spreads into a thin film when it touches an extremely hydrophilic surface. Figure 6a demonstrates the image sequence of a droplet impinging on the substrate with moderate wettability contrast (consisting of adjacent superhydrophobic and hydrophilic areas) when the droplet offset and releasing height are 1.2 mm and 30.5 mm, respectively. In this case, the droplet slightly touches the hydrophilic area. The time is plotted against the positions of the contact lines of the impinging droplet on superhydrophobic and hydrophilic areas in Figure 6b. Following the initial symmetrical spreading stage (2.3 ms), the contact line of the impinged droplet on the superhydrophobic area recoils while it is pinned on the hydrophilic area (10.6 ms and 14.3 ms). The contact line on the superhydrophobic area continues to recede until it reaches the border separating the superhydrophobic and hydrophilic areas (17.1 ms). At this point, the directional rebounding of the droplet happens and the droplet is launched in the lateral direction (26.1 ms). A water droplet impinging on a surface with uniform wettability spreads and recedes symmetrically with no significant net lateral component of the rebounding force (see figures 4 and 5a). On the other hand, an impinging droplet on a non-uniform surface with contrast wettability shows symmetric spreading, but asymmetric receding. There is a noticeable difference in the contact angle at the two edges of the receding droplet on superhydrophobic and hydrophilic areas (see figure 5b). While the contact line of the droplet on the hydrophilic

surface is pinned, the other contact line on the superhydrophobic surface recedes rapidly with a higher lateral component of force. The net force in the lateral direction imposed by the unbalanced lateral forces from both sides induces this directional rebounding of the water droplet towards the hydrophilic area (see figure 5b).

In Figure 7a and b, the image sequences of the directionally rebounded droplets are shown when the impinging droplets slightly touch the hydrophilic/extremely hydrophilic areas on substrates with moderate and extreme wettability contrasts (droplet offset and releasing height were 1.2 mm and 30.5 mm, respectively). The centroid of the rebounded droplet was tracked by averaging the x and y coordinates of all pixels in the selected droplet using MATLAB. The representative trajectory of the directionally rebounded droplets released at the different heights for both substrates are compared in Figures 7c and d, with the droplet offset fixed at 1.2 mm. Repeated experiments showed a good repeatability in terms of the maximum height and landing distance of directional rebounded droplets with the coefficient of variation (CV) ranged in 1.6 – 9.6 %. Generally, it is observed that for both substrates, as the releasing height of the impinging droplet increases, the landing distance of the directionally rebounded droplet increases. With higher releasing heights, the impinging droplet has more kinetic energy converted from potential energy. Thus, the droplet rebounds with an angle after impingement and moves along a curved projectile path across the substrate before landing. It also can be deduced that the landing distance of droplets released from a fixed height increases with the higher wettability contrast across the border. At a higher wettability contrast, the net force applied on the rebounded droplet with an angle increases, which leads to an increase in its landing distance.

The impinging behavior of a water droplet on the substrate with moderate wettability contrast is illustrated in Figure 8. The portion of the impinging droplets touching the hydrophilic area at the maximum spreading increases from 0.12 to 0.43. When the portion of the impinging droplet touching the hydrophilic area is 0.12, 0.16 and 0.22, directional rebounding of the droplet is observed. For all these three cases, a bridge forms in the droplet and eventually breaks, which causes part of droplet to be directionally rebounded while its other part remains still on the surface. As the portion increases from 0.12 (Figure 8a) to 0.26 (Figure 8c), the landing distance of the rebounded droplet decreases while the size of the droplet remaining on the surface increases. In this situation, a greater amount of kinetic energy of the droplet is dissipated by the more pronounced pinning effect of the hydrophilic areas during impingement. Hence, the impinged droplet has less energy to rebound directionally on the surface and larger droplet remains in contact with the surface. When the portion increases to 0.26 and 0.43 as shown in Figure 8d and e, the pinning effect of the hydrophilic areas at the moment of impinging becomes more significant. Consequently, the droplet no longer retains the sufficient kinetic energy to rebound from the surface due to severe energy dissipation by the increased portion of more wetting surface, i.e., hydrophilic surface, and only moves laterally towards the hydrophilic area without rebounding.

4. Conclusions

Substrates with moderate and extreme wettability contrasts comprising of superhydrophobic/hydrophilic and superhydrophobic/extremely hydrophilic neighboring areas separated by a

borderline were fabricated using a combination of masking, hydrophobic nanoparticle treatment and oxygen plasma treatment. The substrates with moderate and extreme wettability contrasts were used to study the impinging behavior of water droplets on substrates with sharp wettability contrasts. Directional rebounding of water droplets released at different heights was observed for the droplets, which slightly touched the hydrophilic or extremely hydrophilic areas on substrates with moderate or extreme wettability contrasts. The directional rebounding of the impinging droplet was attributed to the net surface tension force applied laterally to the droplet due to the significant difference in the contact angles at the two edges of water droplet during the receding stage. For both substrates, as the releasing height of the impinging droplet increases, the landing distance of the directionally rebounded droplet increases because of the enhanced kinetic energy. At a fixed releasing height, the increase in the wetting contrast across the border increases the force applied laterally on the droplet, leading to a further landing distance of the droplet. As the impinging location moves toward the hydrophilic area of the substrate with a moderate wettability contrast, the portion of impinged droplet touching the hydrophilic surface increases and the kinetic energy dissipation of impinging droplet becomes more significant. As a result, no droplet separation and directional rebounding is observed and the droplet only moves on the surface towards the hydrophilic area.

Acknowledgments

The authors would like to acknowledge the financial support from the Office of Provost & Vice President for Academic Affairs and the REP program at Texas State University as well as the Donors of the American Chemical Society Petroleum Research Fund (ACS-PRF 57552-ND9).

References

1. van Dam DB, Le Clerc C. Experimental study of the impact of an ink-jet printed droplet on a solid substrate. Physics of Fluids. 2004; 16:3403–3414.
2. Quan YY, Zhang LZ, Qi RH, Cai RR. Self-cleaning of Surfaces: the Role of Surface Wettability and Dust Types. Scientific Reports. 2016; 6
3. Ye Q, Domnick J. Analysis of droplet impingement of different atomizers used in spray coating processes. Journal of Coatings Technology and Research. 2017; 14:467–476.
4. Xie JL, Wong TN, Duan F. Modelling on the dynamics of droplet impingement and bubble boiling in spray cooling. International Journal of Thermal Sciences. 2016; 104:469–479.
5. Yang YS, Kim HY, Chun JH. Spreading and solidification of a molten microdrop in the solder jet bumping process. Ieee Transactions on Components and Packaging Technologies. 2003; 26:215–221.
6. Tsai PC, Pacheco S, Pirat C, Lefferts L, Lohse D. Drop Impact upon Micro- and Nanostructured Superhydrophobic Surfaces. Langmuir. 2009; 25:12293–12298. [PubMed: 19821629]
7. Yarin AL. Annual Review of Fluid Mechanics. Vol. 38. Palo Alto: Annual Reviews; 2006. Drop impact dynamics: Splashing, spreading, receding, bouncing; 159–192.
8. Rein M. Phenomena of liquid drop impact on solid and liquid surfaces. Fluid Dynamics Research. 1993; 12:61–93.
9. Lee M, Chang YS, Kim HY. Drop impact on microwetting patterned surfaces. Physics of Fluids. 2010; 22
10. Malouin BA, Koratkar NA, Hirsa AH, Wang ZK. Directed rebounding of droplets by microscale surface roughness gradients. Applied Physics Letters. 2010; 96
11. Kim S, Moon MW, Kim HY. Drop impact on super-wettability-contrast annular patterns. Journal of Fluid Mechanics. 2013; 730:328–342.

12. Hoshian S, Jokinen V, Franssila S. Robust hybrid elastomer/metal-oxide superhydrophobic surfaces. Soft Matter. 2016; 12:6526–6535. [PubMed: 27418238]
13. Xue CH, Bai X, Jia ST. Robust, Self-Healing Superhydrophobic Fabrics Prepared by One-Step Coating of PDMS and Octadecylamine. Scientific Reports. 2016; 6:27262. [PubMed: 27264995]
14. Shastry A, Case MJ, Bohringer KF. Directing droplets using microstructured surfaces. Langmuir. 2006; 22:6161–6167. [PubMed: 16800671]
15. Yang JT, Yang ZH, Chen CY, Yao DJ. Conversion of surface energy and manipulation of a single droplet across micropatterned surfaces. Langmuir. 2008; 24:9889–9897. [PubMed: 18683962]
16. Vaikuntanathan V, Sivakumar D. Directional motion of impacting drops on dual-textured surfaces. Physical Review E. 2012; 86
17. Sivakumar D, Katagiri K, Sato T, Nishiyama H. Spreading behavior of an impacting drop on a structured rough surface. Physics of Fluids. 2005; 17:10.
18. Kannan R, Sivakumar D. Drop impact process on a hydrophobic grooved surface. Colloids and Surfaces a-Physicochemical and Engineering Aspects. 2008; 317:694–704.
19. Schutzius TM, Graeber G, Elsharkawy M, Oreluk J, Megaridis CM. Morphing and vectoring impacting droplets by means of wettability-engineered surfaces. Scientific Reports. 2014; 4:7.
20. Mock U, Michel T, Tropea C, Roisman I, Ruhe J. Drop impact on chemically structured arrays. Journal of Physics-Condensed Matter. 2005; 17:S595–S605.
21. Lim CY, Lam YC. An investigation into a micro-sized droplet impinging on a surface with sharp wettability contrast. Journal of Physics D-Applied Physics. 2014; 47:12.

Highlights

- The behavior of water droplets impinging on surfaces with extreme and moderate wettability contrasts was investigated experimentally.
- Impinging droplets with slight touch on the more hydrophobic area rebounded directionally toward the less hydrophobic area.
- The higher wetting contrast and releasing height led to the longer landing distance of the directionally rebounded droplet.
- As the portion of the impinging droplet touching the hydrophilic area on a substrate with moderate wettability contrast increased, the droplet only moved towards hydrophilic area without being rebounded.

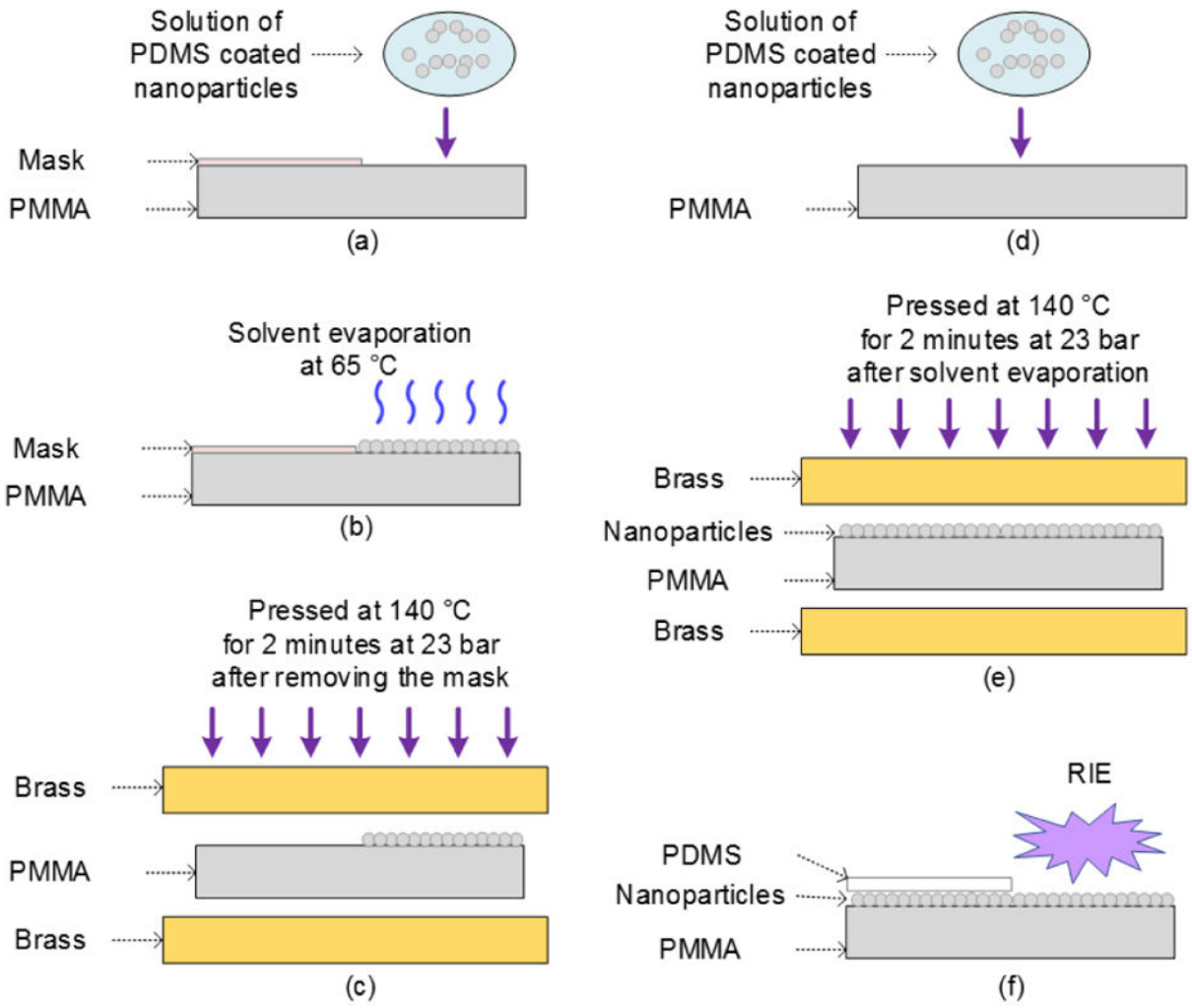

Figure 1.

The process flow diagram for fabrication of PMMA platforms with (a–c) moderate wettability contrast and (d–f) extreme wettability contrast.

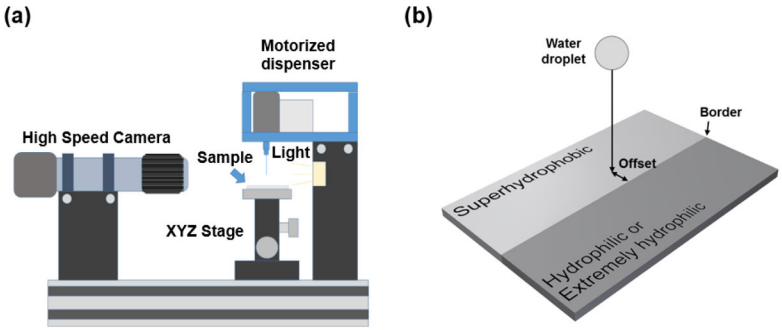

Figure 2.

(a) Schematic illustration of experimental setup to capture image of droplet impinging on surfaces with wettability contrasts and (b) Schematic of a droplet impinging on a platform with moderate/extreme wettability contrasts.

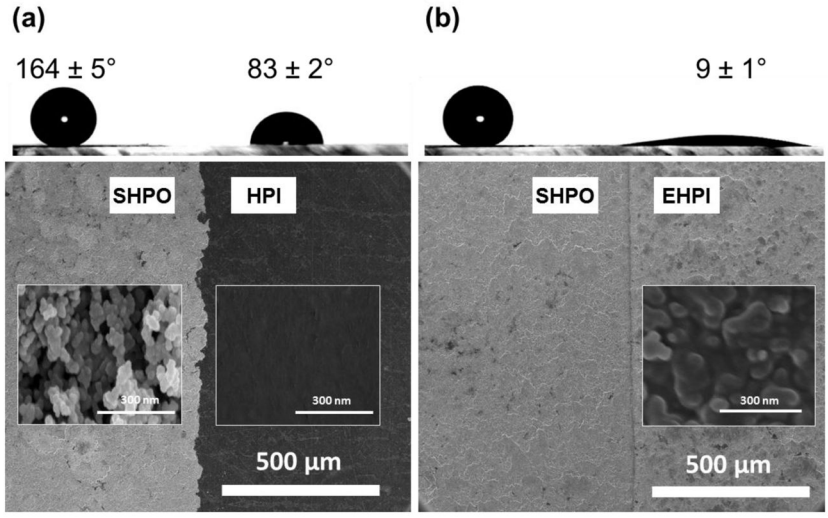

Figure 3.

SEM pictures of the platform with (a) moderate and (b) extreme wettability contrasts. (SHPO: superhydrophobic, HPI: hydrophilic, EHPI: extremely hydrophilic) and water droplets resting on each surface.

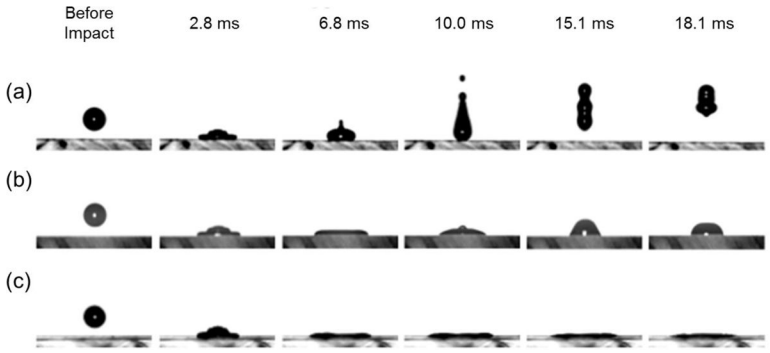

Figure 4.
Water droplets impinging on (a) superhydrophobic, (b) hydrophilic, and (c) extremely hydrophilic substrates.

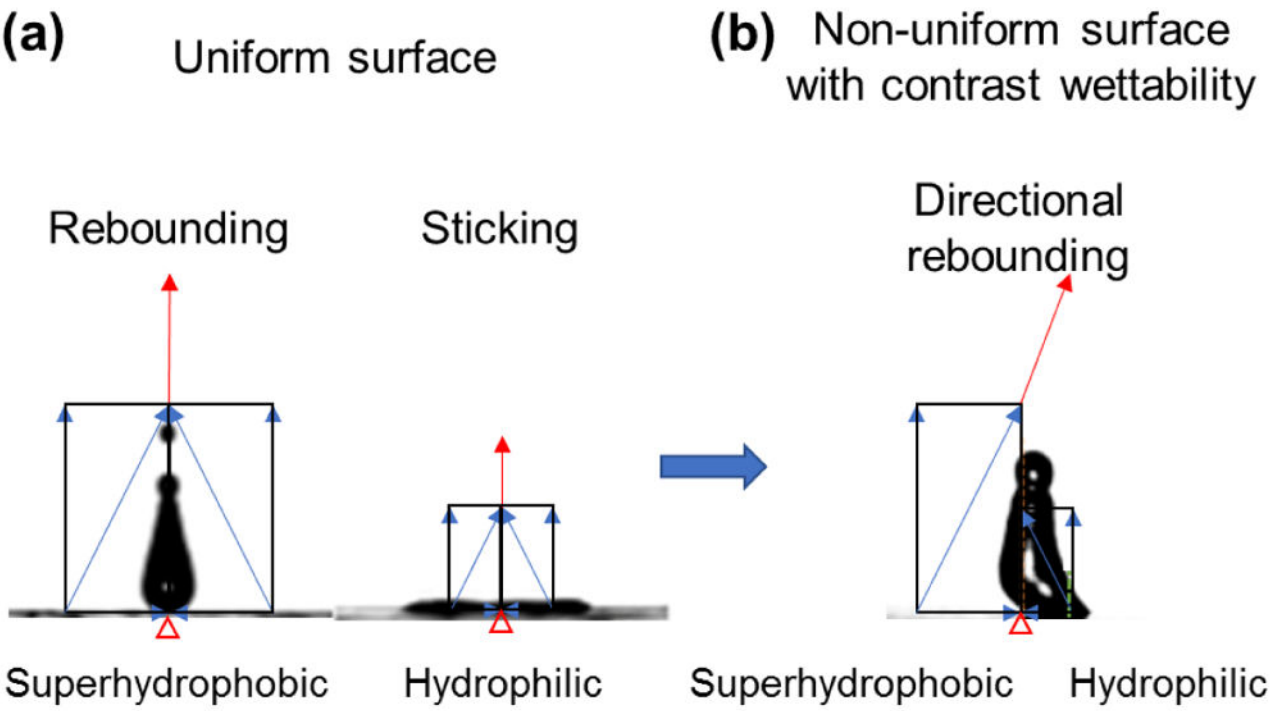

Figure 5.

(a) Rebounding and sticking of impinged droplet on uniform superhydrophobic or hydrophilic surfaces, respectively. (b) Directional rebounding of impinged droplet on non-uniform surface with contrast wettability. Triangle head: the center of impinging droplet.

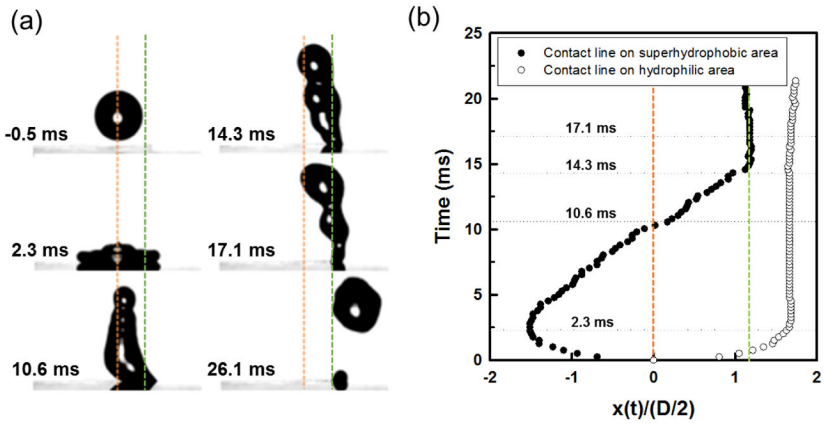

Figure 6.

(a) A water droplet impinging on the surface with a moderate wettability contrast when it slightly touches the hydrophilic area with droplet offset and the releasing heights of 1.2 mm and 30.5 mm (*We* = 18.9), respectively. (b) The contact line trajectory of the impinging droplet on superhydrophobic and hydrophilic areas as a function of time. D: the diameter of droplet before impact; −X(t); contact line distance from the offset (centerline of the impact) on superhydrophobic area; +X(t): contact line distance from the offset on hydrophilic area; orange dot line: offset line (centerline of the impact); and green dot line: border line between superhydrophobic and hydrophilic areas.

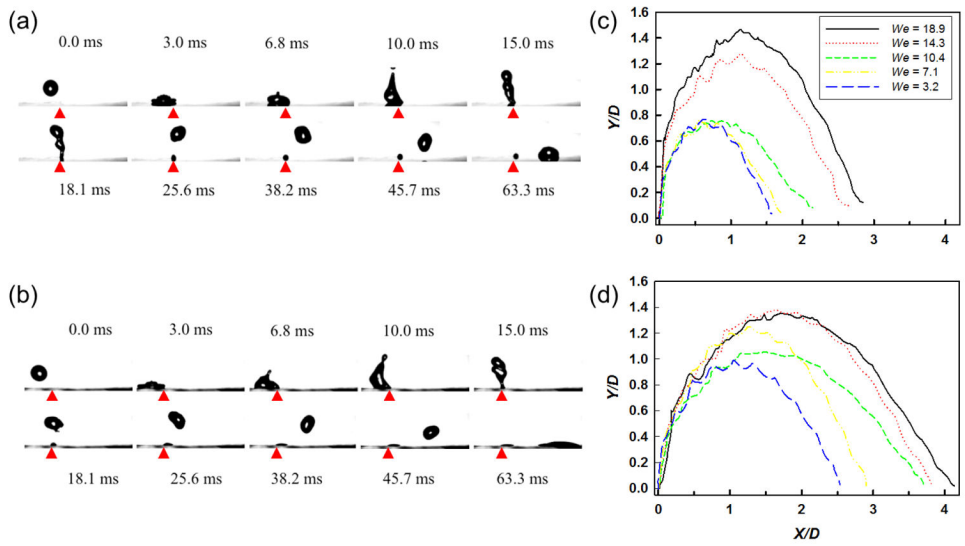

Figure 7.

Directional rebounding of a droplet on surfaces with (a) moderate and (b) extreme wettability contrasts when it slightly touches the hydrophilic/extremely hydrophilic area. The droplet offset and the releasing height were 1.2 mm and 30.5 mm (We = 18.9), respectively. (Red arrow head: border line of wettability contrast) Furthermore, this shows the trajectory of water droplets impinging on (c) moderate and (d) extreme wettability contrasts. The droplet offset was 1.2 mm and the releasing heights were 10.5, 15.5, 20.5, 25.5 and 30.5 mm (We = 3.2, 7.1, 10.4, 14.3, and 18.9).

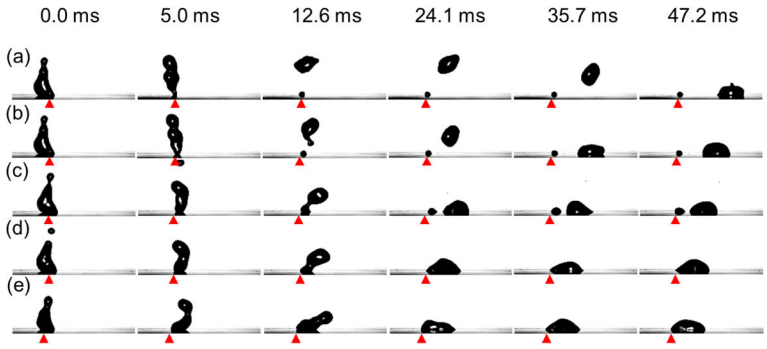

Figure 8.

Impinging behavior of a water droplet on the substrate with moderate wettability contrast when the portion of the impinging droplet touching the hydrophilic area during maximum spreading is 0.12, 0.16, 0.22, 0.26, and 0.43, respectively. The droplet releasing height is 30.5 mm ($We = 18.9$). (Red arrow head: border line of wettability contrast)